

Prediction of Subbase Erosion Caused by Pavement Pumping

A. J. VAN WIJK AND C. W. LOVELL

The characterization of the surface erosion of rigid pavement subbase and shoulder materials is described. Three testing methods were used in the study: (a) a jetting test for unstabilized (noncohesive) materials, (b) a brush test on the effect of six factors on the surface erosion of portland cement- and asphalt-stabilized materials. A statistically designed procedure was used to minimize the number of test samples and to model the interaction of material properties and climatic influences on surface erosion. A number of lean concrete samples were also tested using the brush test; and a rotational shear device was used to obtain the critical shear stress of portland cement-stabilized materials. The brush test provided relative erosion results in terms of weight loss. These results were used to investigate the effects of different variables on the weight loss of stabilized materials and to characterize the erosion of these materials. Brush test results were correlated with rotational shear test results, which were compared with conditions expected to develop under the pavement. The results show that unstabilized materials are not capable of resisting surface erosion in a concrete pavement. Curves were developed for stabilized materials to assist in the selection of subbases and shoulders with low erodibility using standard laboratory tests. These curves include the performance of stabilized materials in different climatic conditions.

Rigid pavement pumping is one of the leading causes of rigid pavement failure. Rigid pavement pumping is defined as (a) the ejection of water and subgrade, subbase or shoulder material through pavement joints, cracks, and edges; or (b) the redistribution of material underneath the slab. The major cause of material removal from the layer can be pore water pressure buildup or surface erosion. Fines are removed from stabilized layers and unstabilized shoulders mainly by surface erosion. In this process water is accumulated under curled slabs at joints. With the deflection of the approach slab the water is pushed toward the leave slab. The leave slab is then deflected very rapidly by the wheel load and the water is pushed back under the leave slab at a high velocity. Fines are then removed from under the leave slab and deposited under the approach slab. This causes the formation of voids and produces faulting.

Voids change the slab support from a uniformly supported to an unsupported condition at some points. Material removed from shoulders by surface erosion can either be ejected along the pavement edge or deposited under the slabs. This causes shoulder depressions and faulting. Fines are removed from unstabilized materials mainly through pore water pressure buildup.

Three conditions are necessary for pumping to occur: (a) high slab deflections (heavy wheel loads, thin slabs, or both);

(b) water in the pavement; and (c) materials that are susceptible to pumping.

Pumping has been a problem in the United States since the 1940s, with the increase in traffic loads during World War II. A number of remedies have been tried to eliminate or reduce pumping. Most of these methods used some type of subbase. Attempts to eliminate pumping include the placement of a granular subbase layer between the slab and the subgrade and the use of stabilized subbases. Stabilized subbases have been used since the 1950s in the United States. These subbases reduced, but did not prevent pumping (1). Lean concrete and asphalt concrete layers have also been used successfully in most cases to prevent pumping, because they are virtually nonerodible.

REVIEW OF EROSION TESTS

Erosion of soil is not only important as a factor in the design of rigid pavements, but also in the design of channels, earth dams, and soil slopes. Erosion occurs as a result of the shear stress induced by water flowing over the soil. Jetting and flume tests have been used extensively to investigate the erosion behavior of different types of soils subjected to flowing water.

The erosion of stabilized materials in channels and dam facings has been studied by subjecting cylindrical and beam samples to water overfalls (2) and jetting (3). Flumes, tube flows, and jetting tests (with jets at different angles) have been used to study the erosion of cohesive and noncohesive soils in geotechnical, hydraulics, and agricultural areas (4–8).

Espey (9) and Moore and Masch (10) developed a rotational shear device in the early 1960s, with which the erosion of cohesive materials could be tested. The apparatus basically consisted of water rotating around a stationary sample. Arulnandan et al. (11) also used a similar device in a study on the erosion of clay materials. Akky and Shen (12) and Akky (13) used such a device to investigate the erosion of soil-cement mixtures. Chapuis (14) improved the device and used it to measure mainly the erosion of cohesive materials.

Various tests have been conducted since the 1940s to investigate pumping. The majority of the U.S. testing programs investigating pumping used full-scale sections (15–19), scaled sections (20), and pavement models (20, 21). The emphasis was on the loss of fines from unstabilized subbase materials.

Although surface erosion is considered an important rigid pavement pumping mechanism, relatively little research has been conducted on the erosion of subbase and shoulder materials.

The California Department of Transportation uses a test referred to as the Surface Abrasion Test to measure the erosion or abrasion resistance of pavement materials (1). The test was

initially developed to study the effect of water action on bituminous mixtures. Researchers in France conducted an extensive investigation on rigid pavement pumping in the late 1970s (22, 23). Four tests were used to evaluate surface erosion: two brush tests, a jetting test, and a vibrating table.

TESTING METHODS

After evaluating a large number of testing procedures, the rotational shear apparatus, a jetting test, and a brush test were chosen to evaluate the erosion of rigid pavement subbases.

ROTATIONAL SHEAR DEVICE

Shear forces on the lateral surface of samples tested with the rotational shear device are uniform, can be calculated, and can be easily changed. The device has been used successfully in the investigation of the erosion of such diverse materials as clays and stabilized materials. The easy adjustment of uniform shear forces makes it applicable to a very wide range of subbase materials. It is the only test in which the shear stress that causes erosion can be measured accurately. The obvious disadvantage of this device is that noncohesive materials cannot be tested.

The rotational shear device was designed to accommodate samples compacted at the size specified in AASHTO T135 (24). The device was designed to have three annular spacings: 9.5 mm (0.375 in.), 13 mm (0.5 in.), and 16 mm (0.625 in.), by using cylinders with different inside diameters. The annular space is defined as the space between the outside of the sample and the inside of the cylinder. The maximum size of the aggregate was set at 9.5 mm (0.375 in.) to allow for the free movement of the eroded material at all times within the annular space. An air motor of 560 W (0.75 hp) was used to rotate the transparent cylinder at speeds of between 300 and 3,000 rpm. A strobe was used to measure the rotational speeds.

The sample was held in place by four 13-mm (0.5-in.) long tubes attached to a thin metal cap and penetrating into the sample. Epoxy was also used to secure samples to a smooth cap when the cap with the tubes could not be used. The sample rested on the bottom cap. Tape was used to protect the ends of the sample by placing it around the top and bottom ends of the sample covering the caps. The tape prevented water from entering the space between the caps and the sample ends. The top cap was connected to a shaft that transferred the rotation due to shear stress on the sample to a lever arm that pressed against a torque measuring device. A load cell, a string and pulley system, and a torque meter were used.

The amount of erosion was measured by recording the weight of the eroded material rather than weighing the sample after each test. This procedure was more cumbersome, but avoided inaccuracies produced by change in degree of saturation during the test, and prevented the sample from being disturbed. The base plate was modified to provide for easy removal of the eroded material. A schematic diagram of the rotational shear device is shown in Figure 1.

A number of tests were conducted to calibrate the equipment. For laminar flows on smooth surfaced samples the shear stresses can be calculated from the rotational speeds. However,

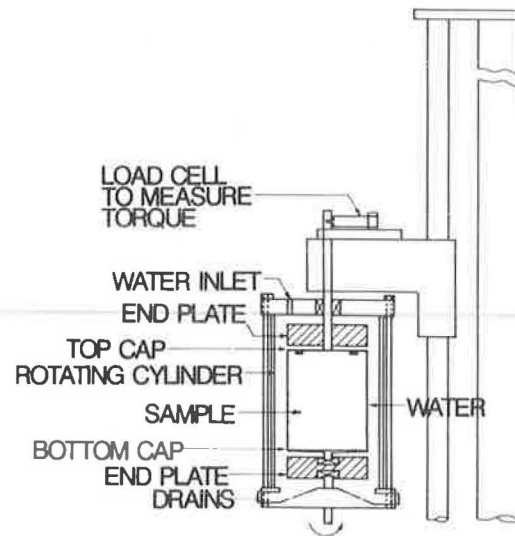


FIGURE 1 Schematic diagram of the rotational shear device.

this condition exists only at very low rotational speeds. The flow of the water in the annular space changes to turbulent flow when the critical Reynolds number (CRN) is reached. The speed at which the CRN is reached depends on the surface roughness of the sample and the annular space. The rotational speeds at which the flows change from laminar to turbulent are about 680 and 820 rpm for annular spaces of 9.52 and 12.5 mm (0.375 and 0.5 in.), respectively (Figure 2). The rate of increase in the shear stress with rotational speed during turbulent flow depends also on the annular space and the sample surface roughness.

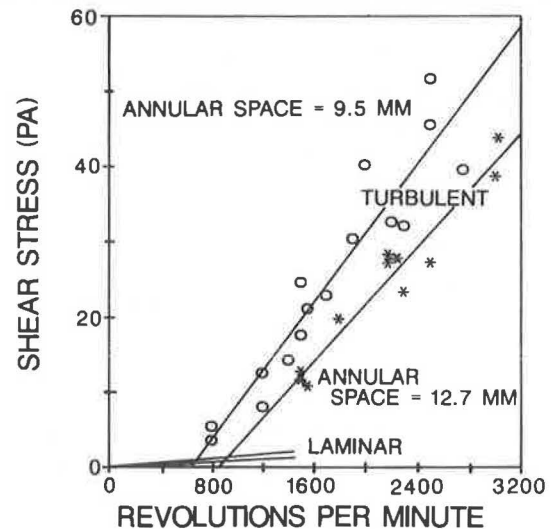


FIGURE 2 Effect of annual space and rotational speed on shear stress.

JETTING TEST

The jetting test (Figure 3) was used to evaluate noncohesive materials. The shear stresses on the sample are not uniform, and cannot be determined as accurately as with the rotational shear test apparatus.

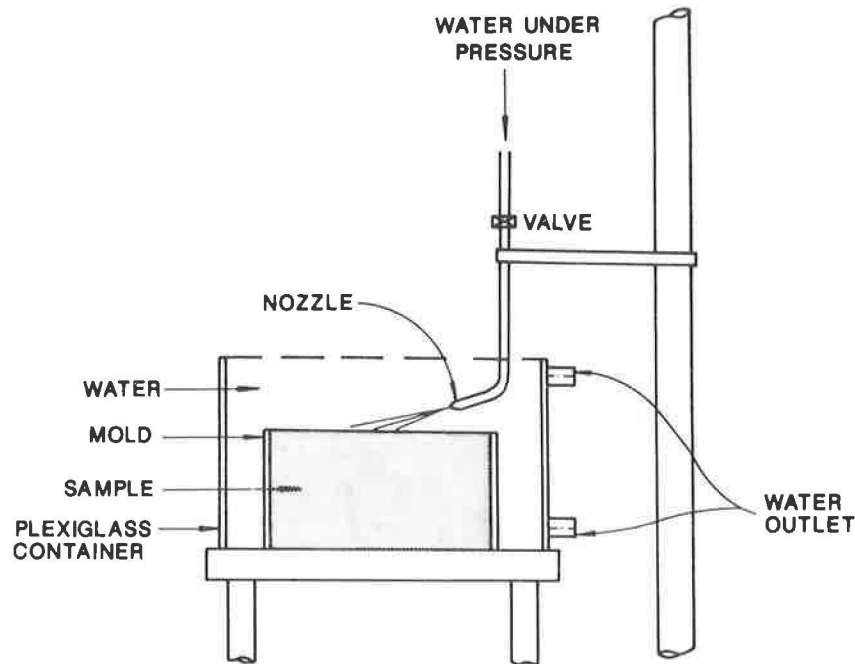


FIGURE 3 Schematic diagram of the jetting device.

The device consisted of a jet placed at an angle of about 20 degrees with the sample. Pressures of up to 345 kPa (50 psi) were provided by a pressure vessel. The sample was placed in a plexiglas container with water outlets at two different levels. Both the pressure vessel and the plexiglas container were built for the study.

The erosion of samples could be measured in the submerged or unsubmerged conditions by changing the water outlet level in the sample container. Samples could also be tested in or out of the molds. Eight spray nozzles with different orifices and spray angles were used. The shear stresses on the sample surface were approximated by dividing the forces at the sample surface by the area of contact. A uniform distribution over the area was assumed.

BRUSH TEST

A brushing test was also selected to evaluate the erodibility of materials, mainly stabilized materials. A brushing test is very simple and fast to use. A large number of samples can be tested, but the results are not correlated to the actual field conditions. The test was therefore selected to be used to investigate the effect of different factors on erosion and to compare the erodibility of materials, rather than trying to correlate the results directly with field conditions. The brush and brushing procedure specified in AASHTO T135 and T136 (24) were used because these procedures are the only standard ones available and are used in the evaluation of cement-stabilized materials.

EXPERIMENTAL PROCEDURES

The purpose of the testing program was to obtain information about the erosion of rigid pavement subbase and shoulder

materials. The variables included in the testing program were chosen to include the properties of most of the subbases used in rigid pavements. This information was obtained from the results of the survey and rigid pavement design procedures, such as the Portland Cement Association (PCA) (25) and AASHTO (26). The results from a survey indicated that portland cement-stabilized, crushed stone, dense-graded, asphalt concrete, sand, and asphalt-stabilized subbases are the most widely used in the United States (27).

Two types of aggregate, pit-run gravel and crushed stone, were selected to represent the unstabilized materials. Portland cement- and asphalt-stabilized materials are most widely used as stabilized layers and were included in the testing program. A limited number of tests were also conducted on lean concrete materials. Asphalt concrete was not included because it is basically nonerodible. The n -value— n is the exponent in the equation $p = (d/D)^n$ where p is the percent passing size d and D is the maximum size—was used to characterize the gradations. Yoder (21) also used the n -value in pumping studies conducted in the 1950s.

The environmental conditions are important factors in determining the performance of all pavement layers. Environmental factors influence the strength, the durability, and the erosion potential of the pavement materials. The most important environmental factors are temperature and moisture content. Changes in temperature can cause freezing and thawing of the pavement materials, while changes in moisture content can cause alternate wet and dry conditions in the materials. Different materials are affected to different extents by these changes, as well as by the number of cycles of each change. The occurrence of the conditions and the number of cycles depend on the geographic location of the pavement and the position of the material in the pavement section. The effect of compaction effort (energy) is important to the strength of the material. The compaction effort would also have an effect on the erosion and was therefore included in the study.

A composite experimental design was selected as a testing procedure because it requires relatively few samples—only 32 samples for five main effects (variables) (28). The effects of the linear main effects can be assessed with an analysis of variants (ANOVA) procedure on the factorial part, and a regression equation can be developed relating the erosion with all main effects (29).

The composite design was used to test the effect of five variables at five levels each for the cement and asphalt-stabilized materials in two separate experiments. The five variables and the levels used are given in Table 1. The variables and levels were selected to include the important factors that influence erosion and the ranges of application of these factors.

A full experimental design was not used for the rotational shear testing; instead, results from the brushing test were used to identify important variables and ranges of these variables. The brushing test results indicated that portland cement content is the most important factor on the erosion. Samples were compacted at six different portland cement contents ranging from 1 to 7 percent because this is the range of portland cement contents at which the largest changes in erosion occur. The shear stresses on the sample are affected by the annular space and the surface roughness of the sample. The surface roughness is a function of the gradation. Samples were therefore also compacted using three different gradations with n -values of 0.3, 0.4, and 0.6.

A number of unstabilized samples were tested to investigate the effect of gradation, plasticity index (PI), and compaction effort on the erosion of these samples by means of the jetting test.

RESULTS

Jetting Test on Unstabilized Materials

The critical water velocity and the shear stress increased with increase in compaction energy, as expected. The compaction effort ranged from Standard Proctor to Modified Proctor. Both the critical water velocity and shear stress increased with an increase in PI. The PI ranged from 1 to 15. Although the jetting device could be used to compare different unstabilized materials, the shear stresses and the erosion cannot be determined very accurately. Assumptions, regarding mainly the area of application, had to be made to obtain some measure of the shear stresses. The calculated critical shear stresses ranged from about 1 to 6 Pa and the water velocities ranged from about 0.75 to 2.5 m/sec (2.5 to 8.2 ft/sec) for the materials tested.

Brush Test on Cement-Stabilized Materials

Although cement- and asphalt-stabilized materials were tested, only the results of the cement-stabilized materials are presented. Erosion was predicted from the average weight loss of the sample after two complete brushes after the last cycle. An analysis of variance was used to evaluate the statistical effects of the variables. All of the main effects and two-way interactions were significant at $\alpha = 5$ percent, except compaction energy and the interaction of gradation n -value and the number of freeze-thaw cycles, which were significant at $\alpha = 10$ percent. The variables are therefore all affected by each other.

TABLE 1 COMPOSITE DESIGN LEVELS

	Factor level					Unit
	-2	-1	0	+1	+2	
X1 CT	0.3	0.4	0.5	0.6	0.7	n -value
AT	0.3	0.375	0.45	0.525	0.6	n -value
X2 CT	86	155	234	313	391	lb. in per in ³
AT	15	30	45	60	75	blows
X3 CT	4	7	10	13	16	% by weight
AT	-1.5	-0.75	0	-0.75	-1.5	% from optimum
X4 CT	0	2	4	6	8	no. of cycles
AT	0	1	2	3	4	no. of cycles
X5 CT	0	2	4	6	8	no. of cycles
AT	0	1	2	3	4	no. of cycles

Note: CT = cement stabilized; AT = asphalt stabilized; X1 = gradation n -value; X2 = compaction effort; X3 = cement or asphalt content; X4 = number of freeze-thaw cycles; X5 = number of wet-dry cycles; and n = exponent in $p=(d/D)^n$, where p is the percentage of material passing size d , and D is the maximum size.

Regression equations were developed to predict the erosion (weight loss) after 7 and 31 days.

A regression equation was also developed to predict the erosion with curing age as one of the variables. Erosion decreased with compaction effort and portland cement content. Erosion was a minimum at a gradation n -value of about 0.5. The erosion increased with the number of freeze-thaw cycles and the number of wet-dry cycles for low cement contents, low compaction efforts, and small gradation n -values. At high cement contents and high compaction efforts, the freeze-thaw and wet-dry cycles had no detrimental effect on the erosion. The variables used are given in Table 2 along with the coefficients, and other properties of the regression equations. The

coefficients of all the variables are given to show the effect of all the variables in the model. Some of these variables can be omitted from the model without reducing the fit drastically. The following reduced equations were obtained:

$$Eb7 = 758.39 - 698.86 \log (X3) \\ (R^2 = 60 \text{ percent})$$

$$Eb31 = 459.88 - 436.59 \log (X3) \\ (R^2 = 72 \text{ percent})$$

$$Ebage = 3.88 - 1.37 \log (X3) - 0.865 \log (\text{age}) \\ (R^2 = 82 \text{ percent})$$

TABLE 2 REGRESSION COEFFICIENTS FOR PORTLAND CEMENT STABILIZED SAMPLES

VARIABLE	COEFFICIENTS		
	Eb31	Eb7	Ebage (log)
constant	1178.1814	1584.2571	2.9552
X1	-1459.7314	-1334.6571	-1.3965
X2	-0.8221	-1.1912	0.009515
X1 ²	973.6656	1589.5526	5.8716
X2 ²	-0.0011	0.0006	0.0000
log (X3)	-958.1171	-1455.1376	-1.7628
log (X4)	88.8042	-	-
log (X5)	17.2777	-	-
log (age)	-	-	-0.8727
X1X2	0.9210	-1.6583	-0.0198
X1X3	42.9041	36.6005	0.1836
X1X4	-23.0810	-	-
X1X5	-0.3667	-	-
X2X3	0.0939	0.1846	-0.0002
X2X4	-0.0025	-	-
X2X5	-0.0161	-	-
X3X4	-0.2540	-	-
X3X5	-0.2009	-	-
X4X5	0.7401	-	-
UCS	-	-	-
UCS ²	-	-	-
R ²	86%	73%	86%
Adj. R ²	81%	70%	85%
Std. error	67.25	152.88	0.125
Coef. var.	63.3%	76.4%	10.9%
n	68	84	194

Note: $Eb7$ = brush erosion after 7 days moist curing (g/m^2); $Eb31$ = brush erosion 31 days after compaction (g/m^2); $Ebage$ = brush erosion with age as a variable (g/m^2); X1 = gradation n -value (0.3 to 0.7); X2 = compaction energy (86 to 391) ($lb\text{-in./in.}^3$); X3 = Portland cement content (1 to 16) with percentage by weight; X4 = number of freeze-thaw cycles (0 to 8); X5 = number of wet-dry cycles (0 to 8); and n = exponent in $p=(d/D)^n$, where p is the percentage of material passing size d , and D is the maximum size.

where

- Eb7 = brush erosion after 7 days moist curing,
 Eb31 = brush erosion 31 days after compaction,
 Ebage = brush erosion with curing age as variable,
 X3 = portland cement content, and
 Age = curing age.

The 32 samples, tested as part of the composite design procedure used pit-run gravel as aggregate. A number of samples were also tested to investigate the effect on erosion of the use of crushed stone as aggregate. No difference in weight loss characteristics could be detected between gravel and crushed stone-stabilized samples, and the results were pooled in the development of the equations.

The unconfined compressive strength (UCS) of the samples was also obtained after 31 days. An equation was developed to predict erosion (as weight loss measured from the brush test) from the 31 day UCS:

$$\log(\text{Eb31}) = 2.9241 - 0.00085 \text{ UCS} + 0.000000112(\text{UCS})^2$$

where

- (Eb31) = brush erosion 31 days after compaction (g/m²), and
 UCS = unconfined compressive strength (psi).

Brush Test on Asphalt-Stabilized Materials

The erosion was predicted from the average weight loss of two brushings after the last cycle, with the sample in a semiwet condition.

The procedure of analysis used for the portland cement-stabilized material was also used for the asphalt-stabilized material. Of the main effects, compaction effort, asphalt content and number of wet-dry cycles were significant at $\alpha = 5$ percent. A number of regression equations to predict the erosion (weight loss) based on the test results were developed. Regression coefficients and ranges of variables used in the development are given in Table 3. A regression equation was also developed to predict the erosion with curing age as one of the variables (Table 3).

The following reduced models were obtained:

$$\begin{aligned} \text{Eb4} &= 209.69 - 116.98 \log(X2) + 149.44(X3) \\ &+ 281.05(X1)^2 - 395.59(X1)(X3) \\ (R^2 &= 72 \text{ percent}) \end{aligned}$$

$$\begin{aligned} \text{Eb16} &= 336.12 - 139.18(X1) - 140.8 \log(X2) \\ &+ 3522277(X5)^2 - 15540.2(X3)(X5) \\ (R^2 &= 61 \text{ percent}) \end{aligned}$$

$$\begin{aligned} \text{Ebage} &= 290.17 - 92.86 \log(X2) + 72.10(X3) \\ &- 110.69 \log(\text{age}) - 192.49(X1)(X3) \\ (R^2 &= 83 \text{ percent}) \end{aligned}$$

where

- Eb4 = brush erosion 4 days after compaction (g/m²),
 Eb16 = brush erosion 16 days after compaction (g/m²),
 Ebage = brush erosion with age as variable (g/m²),
 X1 = gradation *n*-value,
 X2 = compaction energy (Marshall hammer blows),
 X3 = asphalt content (percentage from optimum),
 X5 = number of wet-dry cycles, and
 age = age after compaction (days).

The erosion (weight loss) reached a minimum at a gradation *n*-value of about 0.5. Low compaction efforts and small gradation *n*-values increased the erosion at all levels. The effect of the freeze-thaw cycles was in general small and not significant. At low asphalt contents the weight loss decreased slightly with an increase in the number of freeze-thaw cycles, while at high asphalt contents the weight loss increased slightly with an increase in the number of freeze-thaw cycles.

Asphalt-stabilized materials are subject to stripping, which increases the erosion. Asphalt stripping was simulated in the experimental program by wet-dry cycles because standard tests are not available to simulate stripping conditions with time. The results show that the weight loss of the samples is significantly influenced by these cycles, but it is not clear how well the wet-dry cycling simulated stripping conditions. The weight loss increased with the number of wet-dry cycles in all cases tested, but the rate of increase was higher at low asphalt contents, smaller size aggregates, and low compaction efforts. The weight loss (stripping) decreased as asphalt content increased. The erosion (weight loss) of the asphalt-stabilized samples decreased with age and asphalt content.

Rotational Shear Test on Portland Cement-Stabilized Materials

The erosion of portland cement-stabilized samples was evaluated with cement content as the only variable. A number of parameters may be obtained from the results. Typical results are shown in Figure 4 and the results of the tests are given in Table 4. A rate of erosion before the critical shear stress (T_c) is reached, and the rate after T_c can be obtained. The critical shear stress was defined as the shear stress of the water on the sample at which significant erosion begins. Two straight lines were visually plotted to obtain the erosion rates and the value of T_c . Exponential regression curves were also calculated. The exponential regression may be used to predict the erosion, based on the shear stress, but cannot be used to identify T_c .

The curing age obviously has an influence on the erosion. Samples were tested after different curing ages. Results of tests conducted at different curing times on one sample are shown in Figure 5. The critical shear stress increased with curing age. The erosion rates showed differences, but a statistical correlation could not be identified. The differences were small, in general, and the erosion rates appeared to be almost constant within the curing ages incorporated in the testing program (7 to 31 days).

TABLE 3 REGRESSION COEFFICIENTS FOR ASPHALT STABILIZED SAMPLES

VARIABLE	COEFFICIENTS		
	Eb16	Eb4	Ebage
Constant	646.5860	537.0200	511.6115
X1	-1775.8868	-1553.7052	-634.9318
X2	-	-5.9968	-
X3	47.9811	18.2000	69.2456
X4	61.2182	-	-
X5	25.1490	-	-
X1 ²	1807.8486	1650.9968	707.6971
X2 ²	-	0.0290	-
X3 ²	9.2881	8.5796	3.6533
X4 ²	-1.0083	-	-
X5 ²	3.0548	-	-
log (X2)	-167.3990	-	-174.1663
log (age)	-	-	-102.2842
X1X2	4.1211	4.7099	1.9436
X1X3	-219.7609	-293.3122	-192.4926
X1X4	-76.9163	-	-
X1X5	-10.9880	-	-
X2X3	0.6593	0.2215	0.0635
X2X4	-0.4464	-	-
X2X5	-0.3365	-	-
X3X4	14.2844	-	-
X3X5	-18.6797	-	-
X4X5	-1.6376	-	-
R ²	90%	79%	66%
Adj. R ²	75%	71%	63%
Std. error	22.7994	22.5976	22.2979
Coef. var.	36.3%	29.5%	48.0%
number	33	33	109

Note: Eb4 = brush erosion 4 days after compaction (g/m²); Eb16 = brush erosion 16 days after compaction (g/m²); Ebage = brush erosion with age as a variable (g/m²); X1 = gradation *n*-value (0.3 to 0.6); X2 = compaction energy (15 to 90) from Marshall hammer blows; X3 = asphalt content (-1.5 to 1.5), percentage from optimum; X4 = number of freeze-thaw cycles (0 to 4); X5 = number of wet-dry cycles (0 to 4); and *n* = exponent in $p=(d/D)^n$, where *p* is the percentage of material passing size *d*, and *D* is the maximum size.

The effect of erosion time on erosion rate was also investigated. The erosion rate was found to be a function of a reference erosion rate and the logarithm of time. An erosion time of 10 min was selected as the reference time.

$$E_r = 1.095 + 0.88 * E_{10} + 1.0032 * \log (t)$$

R² = 84 percent, adjusted R² = 80 percent, and *n* = 11

where

$$\begin{aligned} E_r &= \text{erosion rate (g/m}^2\text{·min),} \\ E_{10} &= \text{erosion rate after 10 min (g/m}^2\text{·min), and} \\ t &= \text{erosion time (min).} \end{aligned}$$

The equation is only valid for erosion times of approximately more than 5 min. The weight losses of the samples at small

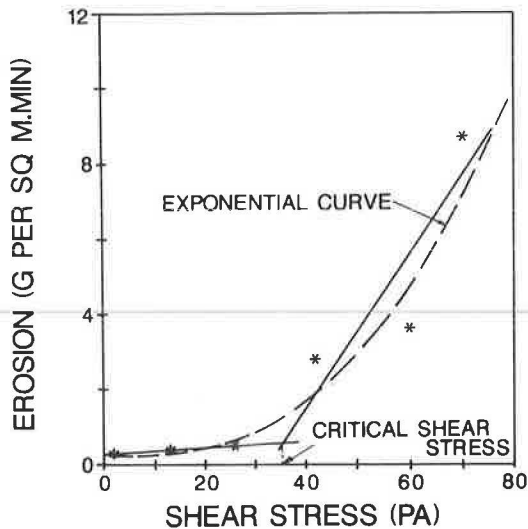


FIGURE 4 Typical rotational shear test results.

erosion times (approximately less than 5 min) were not measured, and therefore cannot be predicted by the equation.

All of the parameters given in Table 4 were compared with each other. The most useful and significant comparisons were critical shear stress and portland cement content. A regression equation was developed to relate the critical shear stress to the brush erosion (weight loss). Critical shear stresses are com-

pared with brush weight loss results in Figure 6. The regression equation has an adjusted R^2 value of 61 percent and is given as follows:

$$T_c = 57.517 - 18.4 * \log(E_b)$$

$$R^2 = 64 \text{ percent, } n = 13$$

where

$$T_c = \text{critical shear stress (Pa),}$$

$$E_b = \text{brush weight loss (g/m}^2\text{).}$$

The materials tested included three different gradations, but no significant differences in T_c of the samples could be detected with the different gradations.

The rotational shear testing has a major limitation in that unstabilized cohesionless materials cannot be tested this way. For example, it was found that samples with cement contents of less than 1 percent had insufficient cohesion for testing in this device.

Brush Test on Lean Concrete Materials

Loss of weight of lean concrete materials depends largely on the portland cement content and the water-cement (W/C) ratio.

TABLE 4 RESULTS OF ROTATIONAL SHEAR TESTS ON PORTLAND CEMENT STABILIZED SAMPLES

Cement con- tent (%)	Curing time (days)	Erosion rate 1	Critical Shear Stress	Erosion rate 2	Brush erosion (g/m ² min)	a	b
1	7	-	4.5	2.04	817	-	-
2.5	7	-	5.5	0.074	265	-	-
	21	0.183	11.0	0.376	155	0.0508	-0.527
3.0	7	-	10.0	-	552	-	-
	31	0.108	13.0	2.76	331	0.0432	0.185
3.0	7	-	7.0	0.104	839	-	-
	31	0.167	12.0	4.0	486	0.1037	-0.683
4.0	7	-	6.0	0.18	309	-	-
	21	0.004	14.0	0.074	155	0.0174	-0.408
	31	0.019	24.0	0.19	66	0.0260	-0.804
7.0	7	-	6.0	0.18	199	-	-
	21	0.011	26.0	0.16	88	0.0229	-0.703
	31	0.011	33.0	0.16	66	0.0218	-0.627

Note: Erosion Rate 1 = erosion rate before T_c (g/m² · min/Pa); Erosion Rate 2 = erosion rate after T_c (g/m² · min/Pa); a, b = coefficients in $\log(\text{erosion}) = a * T + b$; T_c = critical shear stress (Pa); T = shear stress (Pa); 1 kPa = 0.145 psi; 1 m = 3.281 ft; and 1 kg = 2.205 lb.

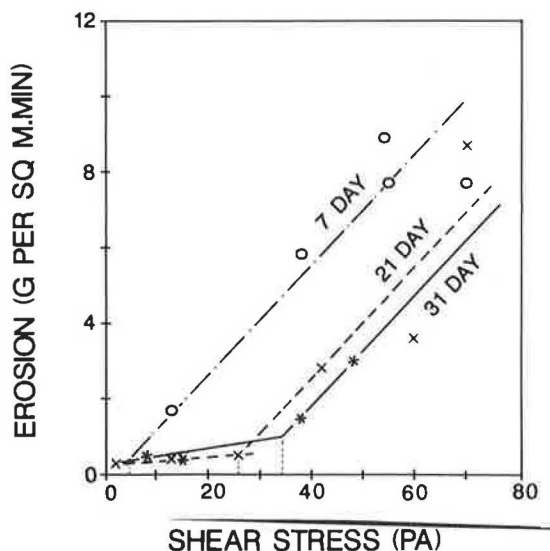


FIGURE 5 Change in critical shear stress with curing time.

The major advantage of lean concrete materials, with regard to erosion, is that loose particles are not as prevalent on the surface as in the case of portland cement-stabilized materials because of the type of compaction. The type of erosion caused by the bristles of the brush makes it impossible to detect differences due to compaction method on the surfaces of the samples. The weight losses induced by the brush bristles on the lean concrete samples were in the same order as those of the cement-stabilized samples.

CORRELATION WITH PAVEMENT CONDITIONS

The laboratory results need to be related to the actual behavior of the pavement to be useful in improving the design of subbases and shoulders. Water between the slab and subbase generates the surface erosion of the subbase or shoulder when the movement of the slab forces the water out of the void at high

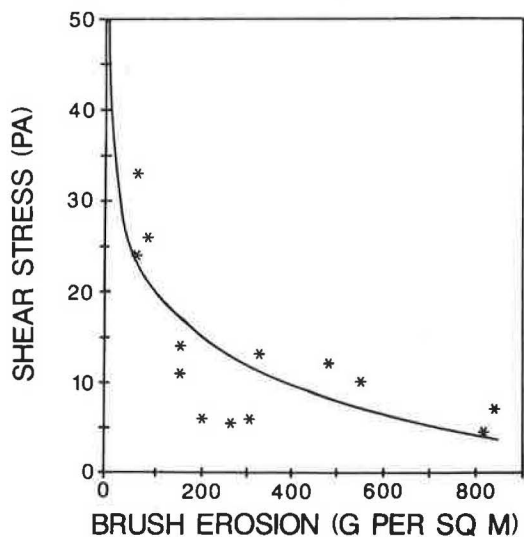


FIGURE 6 Critical shear stress versus brush erosion.

velocities that induce high shear stresses. Little is known about the flow characteristics of water between the slab and an essentially impervious subbase. The flow of the water under the slab is complex and influenced by a number of factors such as slab deflection velocity, the magnitude of the deflections, and void dimensions. At small void thicknesses, the water will resist the slab deflection.

During the late 1970s, French researchers (22, 23, 30) investigated the flow of water on impervious subbases. In their theoretical calculations of the velocity of the water under the slab, they identified three void thickness zones in which water behaves differently. These zones were selected based on theoretical, laboratory, and in-situ observations.

1. Voids less than 0.5-mm (0.02-in.) thick—water behaves as a viscous fluid in these very thin layers.
2. Voids larger than 1-mm (0.04-in.) thick—water behaves as an ideal fluid in these voids.
3. Voids between 0.5- and 1-mm (0.02- to 0.04-in.) thick—this was identified as the transition zone where the fluid is neither ideal nor viscous.

The French results and hydraulic principles were used to obtain the water velocities and shear stresses induced by the water on the subbase under the slab. The slab movement was simulated by a flat, stiff plate rotating around an axis. This is a fair representation of the movement of the leave slab at the joint when the wheel load moves from the approach slab onto the leave slab. The water velocity was expressed as a parabolic distribution:

$$V = A(u/\delta)^2 + B(u/\delta) + C$$

At

$$y = 0, u = 0$$

Thus

$$C = 0$$

At

$$y = \delta, u = V_z\theta \text{ (for small angles)}$$

Thus

$$B = V_z\theta - A.$$

Further

$$\delta u/\delta x + \delta v/\delta y = 0$$

Thus

$$V = - \int (\delta u/\delta x) dy,$$

But

$$V = -V_z \text{ (for small angles)}$$

Solving for A and B:

$$A = -V_Z (3\theta + 1/\theta)$$

$$B = V_Z (4\theta + 1/\theta)$$

The water velocity:

$$\mu = A (y/\delta) + B (y/\delta)$$

The shear stress:

$$\tau = \mu [(2Ay/\delta^2) + B/\delta]$$

where

- v = water velocity in the y-direction,
- u = water velocity in the x-direction,
- δ = void thickness,
- θ = angle between the slab and the subbase,
- μ = kinematic viscosity of water,
- V_Z = speed of slab deflection, and
- t = time.

These equations are true only when the water behaves as an ideal fluid. At very small void sizes the resistance of the water on the downward movement of the slab becomes important. Pnu (23) indicated that the minimum void thickness (after the slab deflection) for which the given equations can be used is about 1 mm (0.04 in.). As mentioned earlier, representative slab deflection velocities and void dimensions have not been established. The void dimensions and slab deflections depend on factors such as wheel load, temperature gradient, slab properties, and load transfer characteristics. The French researchers (23) speculated that the slab deflection velocities range from 1 to 100 mm/sec (0.04 to 4 in./sec).

The slab is not deflected at a constant velocity because it is accelerated from an initial stationary position by the wheel load until the reaction of the water becomes high enough to decelerate the slab to a position of equilibrium. At that position, the downward force of the wheel load is equal to the upward force of the water on the slab. This occurs at small void thicknesses where the viscous effect of the water becomes significant.

The French researchers (23) predicted a maximum water velocity under the approach slab, and between the approach slab and the shoulder of 2.8 m/sec (9.2 ft/sec). The maximum water velocity under the leave slab was predicted to be 4.4 m/sec (14.4 ft/sec). Materials erodible at a water velocity of 5 m/sec (16.4 ft/sec) were classified very erodible, and materials not erodible at a water velocity of 50 m/sec (164 ft/sec) were classified nonerodible. The influence of void size and slab deflection velocity on the shear stress is shown in Figure 7. These values are plotted from the equations for shear stress derived earlier (solid line), and from the French (22) results (dashed line). The shear stress induced by the water was used to describe the effect of the water on the subbase rather than the water velocity because the shear stress is better defined than the water velocity (average, bottom, maximum), and the rotational shear test provides shear stress values. The void length was taken as 0.75 m (2.46 ft), which can be considered a typical

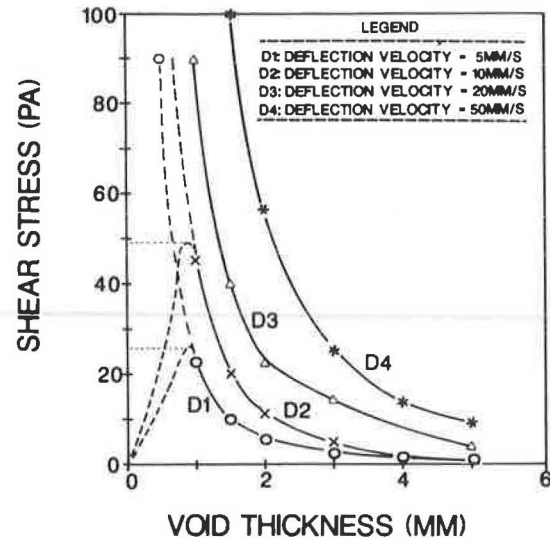


FIGURE 7 Effect of void size and velocity of slab deflection on the shear stress.

length of void at the joint. Both the water velocities and shear stresses increase rapidly at small void thicknesses. Infinitely high water velocities or shear stresses will not be reached because the reaction of the water at small void thicknesses will reduce the slab deflection and velocity of movement, as discussed previously.

Two shear stress values, 25 and 50 Pa (0.52 and 1.04 psf), were selected, based on the previously discussed experimental erosion results (Figures 6 and 7) data presented by the French researchers (22), to distinguish among erosion levels. A material that can resist erosion at a shear stress of 50 Pa (1.04 psf) should not show any signs of erosion during the life of the pavement. A material with a critical shear stress between 25 and 50 Pa (0.52 and 1.04 psf) should experience low erosion, while materials with critical shear stresses lower than 25 Pa (0.52 psf) should be subject to high erosion. The shape of the shear stress weight-loss curve (Figure 6) indicates that the weight loss drops off significantly at shear stresses of less than 20 to 25 Pa (0.42 to 0.52 psf). It must be emphasized that these values have not been verified and are provided only as a guideline.

DESIGN TO MINIMIZE EROSION

Unstabilized Materials

The shear stresses induced by the water (Figure 6) are likely to be higher than the T_c of the unstabilized materials. Therefore, any impervious unstabilized material used in rigid pavements will erode. The critical shear stress can be increased by increasing the compaction effort and the PI of the material, but it will probably not be sufficient to prevent pumping.

Unstabilized materials are subject to more than surface erosion. In most unstabilized materials, pumping is a combination of pore water pressure buildup and surface erosion. The more permeable the materials, the lesser the impact of surface erosion on pumping. The permeability at which the pore water

pressure buildup becomes more important was not addressed in this study.

Stabilized Materials

Stabilized materials are usually relatively impervious and primarily subject to surface erosion. Stabilized materials can be strong enough to withstand surface erosion forces under the slab, depending on the composition of the material and environmental conditions.

The result of erosion testing will be most useful if the large number of variables and combinations of variables included in the testing program can be condensed to a few representative cases. This was done by identifying four climatic regions and four typical gradation-compaction effort combinations. The climatic regions were adapted from a map prepared by Carpenter et al. (31) and are shown in Figure 8. The laboratory tests were conducted to simulate four climatic conditions (warm dry, warm wet, cold dry, and cold wet) by using combinations of wet-dry and freeze-thaw cycles. The conditions in the wet regions (I) were simulated by eight wet-dry cycles and the freeze (A) and freeze-thaw (B) regions by eight freeze-thaw cycles.

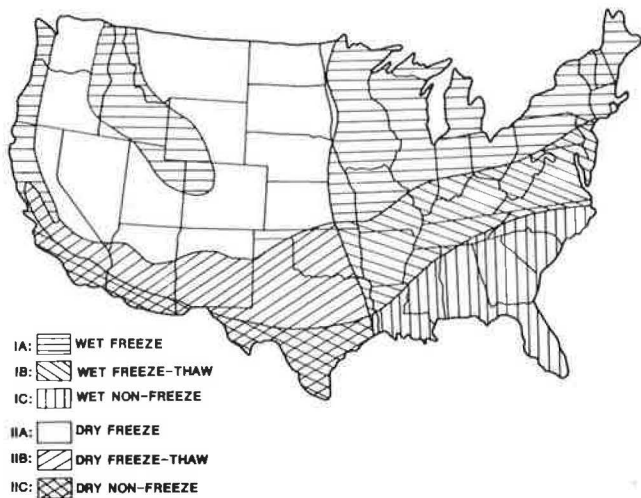


FIGURE 8 Climatic regions in the United States.

The weight loss or brush erosion was normalized to the erosion of a granular material stabilized with 3.5 percent cement, a gradation *n*-value of 0.5, and compacted with an energy of 234 lb-in./cu in. The erosion of this sample was chosen based on the study by Pnu and Ray (22). Results for the portland cement-stabilized materials are shown in Figures 9-12. From these relationships a portland cement content can be selected to ensure low erosion for each one of the four typical gradation-compaction effort combinations for each of the four climatic regions. The selection of a limiting shear stress or erosion level is still an open question. The value of 25 Pa (0.52 psf), recommended in the preceding section, can be used as a guideline in design of subbases and shoulders. A critical shear stress of 25 Pa (0.52 psf) corresponds with a brush erosion of about 60 g/m²-min and a normalized brush

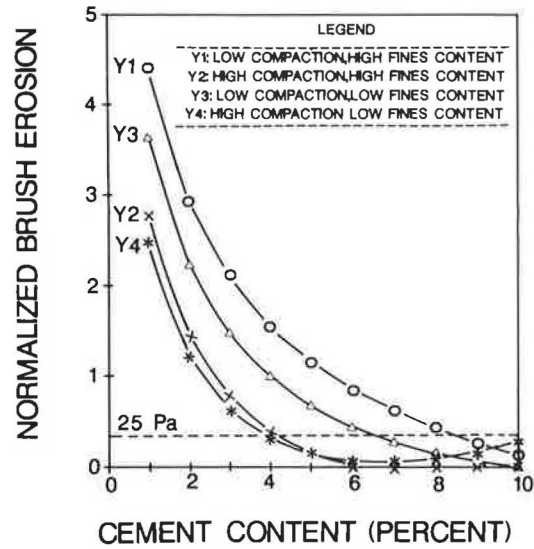


FIGURE 9 Erodibility of portland cement stabilized material in a warm, dry climate.

erosion of 0.33. A shear stress of 50 Pa (1.04 psf) corresponds to a brush erosion of about 3 g/m²-min and a normalized brush erosion of 0.02. The curves can serve as a guideline in the design of rigid pavement subbases and shoulders.

Lean Concrete Materials

One of the characteristics of a stabilized layer is the existence of loose material on the surface after construction. These loose particles will erode regardless of the portland cement or asphalt content. Some of these particles can be removed by sweeping the surface of the subbase. The effect of construction on the erosion could not be included in the testing program, and is therefore not included in the erosion values presented in this paper. Indications are that the erosion of lean concrete materials will be approximately the same as the erosion of cement-

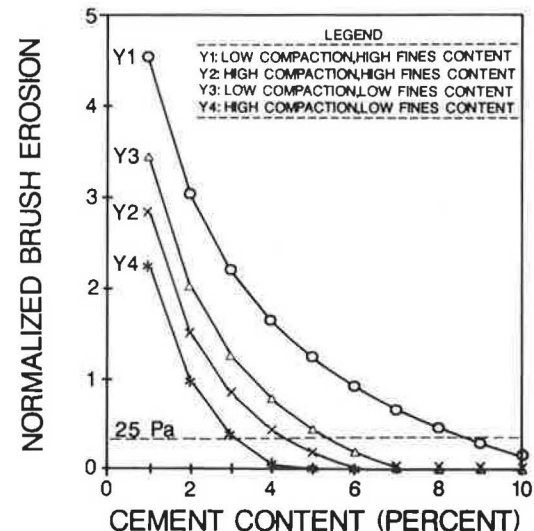


FIGURE 10 Erodibility of portland cement stabilized material in a cold, dry climate.

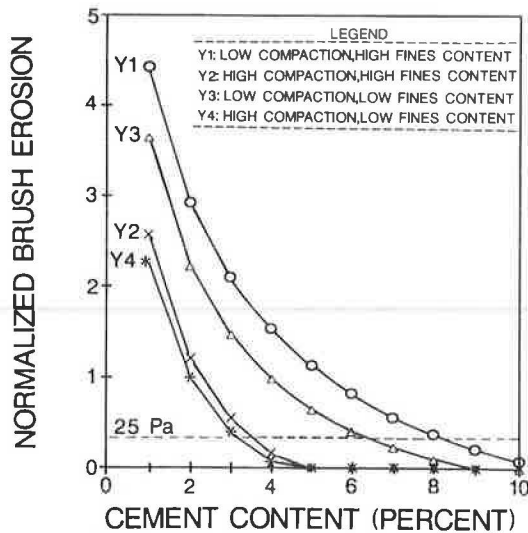


FIGURE 11 Erodibility of portland cement stabilized material in a warm, wet climate.

stabilized materials with the same portland cement content. Ray et al. (32) reported that a portland cement-stabilized material with 3 percent cement will be 7 times more erodible than a lean concrete material with 7 percent cement. The same order of difference in erosion between materials stabilized with 3.5 and 7 percent portland cement is shown in Figures 9–12.

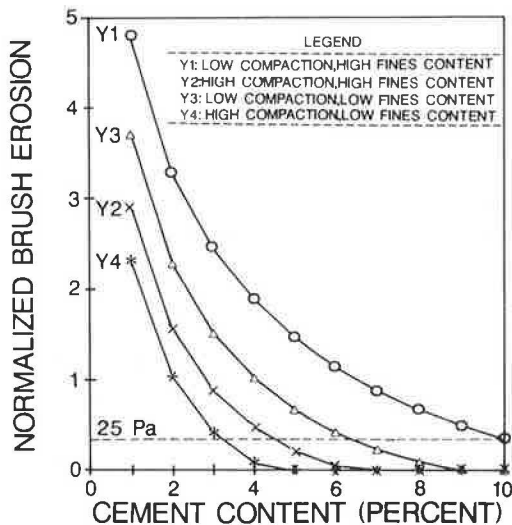


FIGURE 12 Erodibility of portland cement stabilized material in a cold, wet climate.

CONCLUSIONS

The brush test was appropriate for comparing the erosion of different lean concrete samples, but was inappropriate for comparing the effect of the different compaction efforts used in preparing lean concrete and cement-stabilized samples on erosion.

Use of the jetting test to characterize the erosion of unstabilized materials was the least successful. Although differences in erosion among unstabilized samples could be

detected, the accuracy of the calculated and measured shear stresses are suspect.

Use of the rotational shear device was successful for determining the critical shear stresses and erosion rates of portland cement-stabilized materials. A relationship was developed between the brush erosion and the critical shear stress determined from the rotational shear test.

Portland cement content is the most important factor in the erodibility of cement-stabilized materials. The compaction effort and gradation are also important, but to a lesser extent. Environmental factors, such as freeze-thaw and wet-dry cycles, are only important when (a) the cement content is low, (b) the compaction effort is low, and (c) the material contains a large percentage of fines.

The results of the laboratory tests in asphalt-stabilized samples were not presented in this paper, but a summary of the main results is provided. The erosion of asphalt-stabilized materials is affected by the asphalt content, the compaction effort, and environmental factors. Wetting and drying have greater influence on the erosion of asphalt-stabilized materials than freezing and thawing.

The relationships of the brush erosion of asphalt and portland cement-stabilized materials to three material properties and two environmental factors were developed. These relationships can be used to predict the erosion of existing stabilized subbases or to design subbases with low erosion properties.

Indications are that the shear stresses induced by water under the slab are higher than the critical shear stress for unstabilized samples. Therefore, impervious unstabilized materials will always be affected by the pumping resulting from surface erosion. In less impervious unstabilized layers, the pore water pressure buildup is the controlling pumping mechanism.

Stabilized materials that may be eroded in a pavement, depending on their properties, are mainly the asphalt and portland cement contents. A family of curves was developed for four gradation-compaction effort combinations in each of four climatic regions, relating the normalized erosion to portland cement. These relations can be beneficial in the selection of rigid pavement subbase or shoulder materials to prevent pumping. Only the surface erosion is included in these curves. The strength and cost of these layers must be considered separately.

The guidelines presented for design have not been field verified, and should therefore be used with care. Further research is necessary, especially on the shear stresses present underneath the slab.

ACKNOWLEDGMENTS

The research was conducted under contract with FHWA with G. Ring as the project monitor. His assistance throughout the project is greatly appreciated. F. Glossic was responsible for building the equipment used in the study. The assistance and advice of Ross Duckworth during the experimental part of the study was invaluable.

REFERENCES

1. J. H. Woodstorm. Erodibility Testing and Development of Lean Concrete Base in California. Presented at International Seminar on

- Drainage and Erodibility at the Concrete Slab-Subbase-Shoulder Interface, Paris, France, March 24-25, 1983.
2. L. L. Litton and R. A. Lohnes. Soil-Cement for Use in Stream Channel Grade-Stabilization Structures. In *Transportation Research Record 839*. TRB, National Research Council, Washington, D.C., 1982, pp. 33-37.
 3. P. J. Nussbaum and B. E. Colley. Dam Construction and Facing with Soil-Cement. In *Research and Development Bulletin*, Portland Cement Association, Skokie, Ill., 1971.
 4. R. N. Bhasin. *Erodibility of Sand-Clay Mixtures as Evaluated by a Water Jet*. MSCE thesis. Purdue University, West Lafayette, Ind., Aug. 1969.
 5. U. Dash. *Erosive Behavior of Cohesive Soils*. Ph.D thesis. Purdue University, West Lafayette, Ind., Jan. 1968.
 6. R. E. Passwell. *Special Report 135: Causes and Mechanisms of Cohesive Soil Erosion: The State of the Art*. TRB, National Research Council, Washington, D.C., 1973, pp. 52-74.
 7. W. H. Graf. *Hydraulics of Sediment Transport*. McGraw-Hill Company, New York, N.Y., 1971.
 8. V. A. Vanoni. Sedimentation Engineering. In *ASCE, Manuals and Reports on Engineering Practice, No. 54*, New York, N.Y., 1975.
 9. W. H. Espey. *A New Test to Measure the Scour of Cohesive Sediment*. Technical Report HYD 01-6301. Hydraulic Engineering Laboratory, Department of Civil Engineering, University of Texas, Austin, Tex., April 1963.
 10. W. L. Moore and F. D. Masch. Experiments of the Scour Resistance of Cohesive Siments. *Journal of Geophysical Research*, Vol. 67, No. 4, April 1962, pp. 1437-1449.
 11. K. Arulanandan, A. Sargunam, P. Loganathan, and R. B. Krone. *Special Report 135: Application of Chemical and Electrical Parameters to the Prediction of Erodibility*. TRB, National Research Council, Washington, D.C., 1973, pp. 42-51.
 12. M. R. Akky and C. K. Shen. *Special Report 135: Erodibility of a Cement-Stabilized Sandy Soil*. TRB, National Research Council, Washington, D.C., 1973, pp. 30-41.
 13. M. R. Akky. *Erodibility of Soil-Cement*. Ph.D. thesis. Department of Civil Engineering, University of California at Davis, Davis, 1974.
 14. R. P. Chapuis and T. Gatién. Quantitative Measurements of the Scour Resistance of Clays. *Canadian Geotechnical Journal*, May 1983.
 15. W. T. Spencer, H. Allen, and P. C. Smith. Pavement Research Project in Indiana. *Bulletin 116*, HRB, National Research Council, Washington, D.C., 1952, pp. 1-56.
 16. C. W. Allen and L. D. Childs. Pavement Research Project in Ohio. *Bulletin 116*, HRB, National Research Council, Washington, D.C., 1955, pp. 57-70.
 17. F. N. Scrivner. *Special Report 73: Structural Deterioration of Test Pavements: Rigid*. HRB, National Research Council, Washington, D.C., 1962, pp. 186-197.
 18. L. D. Childs, B. E. Colley, and J. W. Kapernick. Tests to Evaluate Concrete Pavement Subbases. *ASCE Journal of the Highway Division*, Vol. 83, No. HW3, July 1957, pp. 1297-1; 1297-40.
 19. F. Burggraf. *Special Report 4: Test One-MD*. HRB, National Research Council, Washington, D.C., 1952, 142 pp.
 20. B. J. Dempsey. Laboratory and Field Studies of Channeling and Pumping. In *Transportation Research Record 849*, TRB, National Research Council, Washington, D.C., 1982, pp. 1-11.
 21. E. J. Yoder, J. A. Havers, W. P. Chamberlain, and R. D. Walker. *Base Course Requirements for Rigid Pavements*. Technical Report 183, Cold Regions Research and Engineering Laboratory, Hanover, N.H., Oct. 1966.
 22. N. C. Pnu and M. Ray. The Erodibility of Concrete Pavement Sub-base and Improved Subgrade Materials. In *Bulletin de Liaison des Laboratoires des Ponts et Chaussées, Special Issue 8*, Paris, France, July 1979, pp. 32-45, (in French).
 23. N. C. Pnu and M. Ray. The Hydraulics of Pumping of Concrete Pavements. In *Bulletin de Liaison des Laboratoires des Ponts et Chaussées, Special Issue 8*, Paris, France, July 1979, pp. 15-31, (in French).
 24. *Standard Specifications for Highway Materials and Methods of Sampling and Testing—Part II: Methods of Sampling and Testing*. 10th ed. AASHTO, Washington, D.C., 1970.
 25. *Thickness Design for Concrete Highway and Street Pavements*. Portland Cement Association, Skokie, Ill., 1984.
 26. *AASHTO Interim Guide for Design of Pavement Structures, AASHTO, Chapter III Revised*. AASHTO, Washington, D.C., 1981.
 27. A. J. Van Wijk. *Design to Prevent Pumping: (1) Subbase Erosion and (2) Economic Modeling*. Ph.D. thesis. Purdue University, West Lafayette, Ind., May 1985.
 28. W. G. Cochran and G. M. Cox. *Experimental Design*. 2nd ed. J. Wiley and Sons, New York, N.Y., 1957.
 29. V. L. Anderson and R. A. McLean. *Design of Experiments: A Realistic Approach*. Marcel Dekker, Inc., New York, N.Y., 1974.
 30. M. Ray. Drainage and Erodibility at Contacts Between Concrete Slab, Subbase and Shoulder. Presented at the International Seminar on Drainage and Erodibility at the Concrete Slab-Subbase-Shoulder Interface, Paris, France, March 24-25, 1983.
 31. S. H. Carpenter, M. I. Darter, and B. J. Dempsey. *A Pavement Moisture Accelerated Distress (MAD) Identification System*. RJ-81/079, FHWA, U.S. Department of Transportation, Washington, D.C., 1981.
 32. M. Ray, J. Christory, and J. Poilane. Drainage and Erodibility: International Seminar Synthesis and New Research Results Related to Field Performance. *Proc., Third International Conference on Rigid Pavement*, 1985, pp. 609-624.

The contents of this paper reflect the views of the authors who are responsible for the facts and the accuracy of the data presented here.